Wideband patch array antenna using superstrate configuration for future 5GApplications

Turkish Journal of Electrical Engineering and Computer Sciences

Volume 28 | Number 3 Article 32

1-1-2020

Wideband patch array antenna using superstrate configuration for future 5GApplications

SIDRA FARHAT

FARZANA ARSHAD

YASAR AMIN

JONATHAN LOO

Turkish Journal of Electrical Engineering & Computer Sciences

http://journals.tubitak.gov.tr/elektrik/

Research Article

Turk J Elec Eng & Comp Sci
(2020) 28: 1673 – 1685

doi:10.3906/elk-1910-160

Wideband patch array antenna using superstrate configuration for future 5G applications

Sidra FARHAT[1,*], **Farzana ARSHAD**[1], **Yasar AMIN**[1], **Jonathan LOO**[2]
[1]ACTSENA Research Group, Department of Telecommunication Engineering,
University of Engineering and Technology, Taxila, Pakistan
[2]School of Computing and Engineering, University of West London, London

Received: 23.10.2019 • **Accepted/Published Online:** 17.12.2019 • **Final Version:** 08.05.2020

Abstract: In this work, four distinct antenna configurations for future-centric 5G applications are proposed. Initially, a single rectangular patch is designed to operate at the frequency of 28 GHz while maintaining a wide operational band. Performance of the antenna is improved by incorporating an array of identical rectangular elements resulting in a higher gain and wider bandwidth. The proposed arrangement consists of three rectangular elements realized using 0.508-mm-thick Rogers RT/Duroid 5880 laminate. The bandwidth is further enhanced by increasing the number of radiating elements in the array from three to five. Evolution of the proposed design is concluded by stacking the superstrate layer above the five-element array structure, thereby improving the gain associated with the proposed configuration. The antenna covers the frequency band from 25.1 GHz to 30.5 GHz under consideration for 5G communications. The proposed antenna occupies a physical footprint of 3.5×3.5 cm^2. Performance of the presented antenna configurations is analyzed using different electromagnetic descriptors including bandwidth, reflection coefficient, gain, radiation patterns, and radiation efficiency obtained using Computer Simulation Technology Microwave Studio (CST MWS) software. The measured results, obtained after fabrication and testing, demonstrate good overall agreement with the simulated outcome. The formulated design is a prime candidate for deployment in 5G applications of the future.

Key words: Antenna arrays, microstrip patch, millimeter wave communication, superstrate, wideband, 5G applications

1. Introduction

Rapid advancements in wireless communication systems have piqued the interest of present-day researchers towards higher frequencies. The millimeter-wave (MMW) frequency band can be utilized to achieve more bandwidth to provide high data rate, improved signal quality, and low latency between transmitter and receiver [1]. Another desirable feature of the MMW frequency band is the reduced interference from nearby applications, owing to fewer applications operating at this frequency band [2]. Moreover, the inverse relationship between the wavelength and operational frequency permits achieving design compactness in antenna structures that are suitable for smartphones, tablets, wearable devices, and wireless local area network (WLAN) applications [3]. Licensed bands approved by the Federal Communications Commission (FCC) for fifth-generation (5G) communication are 28 GHz, 37 GHz, 39 GHz, and the unlicensed spectrum ranges from 64 to 71 GHz [4]. 5G communication requires antennas to offer a minimum of 12 dBi gain and 1 GHz bandwidth within the operating frequency band for efficient communication [5].

*Correspondence: sidrafarhat63@yahoo.com

Microstrip patch antennas are extensively used because of their low profile, lighter weight, low cost, ease of fabrication, simple structure, and conformability [6]. However, low gain and narrow bandwidth are the main drawbacks associated with such antennas [7]. Different techniques are adopted to enhance their bandwidth. The most commonly employed technique involves the use of an electrically thick substrate that enhances bandwidth up to 35% but results in spurious radiations and surface waves [8]. However, the spurious radiations of the feed line can be suppressed by using a feed line that bears a relatively thin width. This technique has been implemented in [9]. A cavity backed antenna is designed with the thin substrate used for the patch design. This allows for a narrower design of the feed line, whereas a cavity is introduced within the thick layer of substrate placed beneath the thin substrate. The combination of thin substrate and thick cavity is replaced with artificial magnetic conductors (AMCs) in [10]. It is observed that AMCs, when used as an antenna ground plane, enhance the performance of the antenna by reducing the back radiations. Moreover, the gain and bandwidth are also increased. However, the structure of the proposed design is intricate in terms of being trilayered. It is important to mention that the aforesaid techniques are discussed for low frequencies.

Defected ground structure (DGS) is a common technique used by researchers to enhance the antenna gain and bandwidth and to reduce the harmonics and cross-polarization [11, 12]. However, complex fabrication procedures are involved to introduce narrow slots in either the ground plane or the patch.

Excitation of higher order modes is also considered as a solution for wideband and high gain. In [13], higher order modes are excited through surface modification and introducing slots on patch. As a result, 15.14% bandwidth and a peak gain of 8.5 dBi is achieved for the Ka-band. Higher order modes' excitation using substrate integrated waveguide (SIW) technology is discussed in [14]. A peak gain of 13.8 dBi with a bandwidth of 8.5 GHz is achieved for the MMW band at the cost of an intricate antenna structure. Moreover, excitation of higher order modes leads to high side-lobe levels and unwanted radiation patterns.

A wideband 4 $\times$ 4 multiple-input multiple-output (MIMO) antenna is presented in [15]. The design operates at 2.4 GHz for LTE-A and at 28 GHz for 5G communication. Four MIMO chip antennas are connected to cover the low band and substrate integrated waveguide-Butler matrix (SIW-BM) antenna operates at the 28 GHz band. A frequency band of 27–29 GHz with a peak gain of 9 dBi is achieved for 5G communication. In [16], a wideband antenna array with the square slot is presented for 60 GHz. The discussed design consists of three dielectric substrate layers and four metal layers. Simulated peak gain of 14.2–12.4 dBi is obtained for the frequency band ranging from 57 to 66 GHz. A seven-layer-based wideband antenna array for 5G is presented in [17]. The proposed design achieves a wideband ranging from 26.5 to 38.3 GHz with gain of 15 dBi. The designs mentioned in the preceding discussion have multifaceted structures resulting in fabrication complexities.

Higher frequencies have inherent issues such as high path losses due to significant atmospheric absorption of electromagnetic (EM) waves [11, 18]. High gain antennas have the potential to mitigate this problem [19]. Multiple techniques have been reported in the literature to achieve high gain in antennas including the use of AMCs, electromagnetic bandgap structures (EBGs), superstrates, and arrays. The simplest technique is the use of arrays in which two or more radiating elements are placed with specified interelement spacing to reduce the unwanted mutual coupling and to enhance the constructive interference. Various antenna arrays for 5G have been proposed [20–22]. In [20], an SIW multibeam array is presented for the 30 GHz band and a peak gain of 12.1 dBi with a bandwidth of 4 GHz ranging from 28 to 32 GHz is obtained. In [21], an SIW technology-based antenna array for handset devices is presented. The gain up to 13.97 dBi with a bandwidth of 2.3 GHz is achieved for the 28 GHz band.

A switchable antenna array to provide coverage in the desired direction is designed in [22]. To provide coverage with more than 10 dB gain, three identical subarrays are proposed, and the desired direction of coverage is achieved by switching the feeding network. The overall volume of the antenna is 55 $\times$ 110 $\times$ 4.5 mm^3 and it achieves a bandwidth of 1 GHz ranging from 21 to 22 GHz. In [23], a stacked array of 42 parasitic patch elements for 5G is presented that acquired a frequency band ranging from 26.83 to 28.56 GHz. In [24], a four-element-based dielectric dense patch array antenna for 28 GHz is proposed. For the enhancement of radiation characteristics, the superstrate layer is positioned above the array and an EBG structure is used in the ground plane. The wide bandwidth of 5 GHz is achieved ranging from 27 to 32 GHz with a peak gain of 16 dBi. This, however, is implemented at the cost of a bulky design consisting of two layers in addition to the superstrate, each having a complex design of its own. In [25], a two-arrays-based antenna system is developed that is capable of operating at low-frequency bands (3 GHz and 4 GHz) for fourth-generation (4G) and 28 GHz for 5G. Both arrays are employed on the same layer of a substrate, and bandwidth of 4.9 GHz is achieved with a peak gain of 10.29 dBi for 5G. A wideband, four-elements-based linear array is presented in [26]. Rectangular and circular shaped slots are etched on the array elements to enhance the antenna performance, and a peak gain of 13 dBi is achieved with a bandwidth of 2.05 GHz.

A superstrate layer was typically used as a cover to protect the antenna from environmental hazards. Later, it was discovered that the antenna gain and efficiency can be enhanced using a superstrate layer properly spaced from the radiating patch with optimized parameters [27]. Multiple reflections that occur between the dielectric superstrate and radiating element are responsible for the enhancement of antenna gain [24, 28]. A broadband antenna array using a holey superstrate is proposed in [29], demonstrating that the superstrate layer is responsible for the enhancement of gain, bandwidth, and reduction of side-lobe levels.

In this paper, a wideband patch array antenna using superstrate is proposed for the 28 GHz frequency band of 5G. The antenna design makes use of a single layered grounded array in addition to the superstrate placed at a finite gap instead of the previously proposed trilayered structures. Moreover, the array design consists of identical rectangular-shaped elements implementable involving simple fabrication processes. The compact array design spans 3.5 $\times$3.5 cm^2 and is realized on 0.508-mm-thick Rogers RT/Duroid 5880. A Rogers 4350B-based superstrate layer is spaced at $\lambda/2$ distance from the patch array. The proposed design covers the 5.4 GHz bandwidth of 28 GHz band with a peak gain of 13.4 dBi.

2. Evolution of antenna design

The proposed work involves a multistaged evolutionary process involving improvements of a variety of antenna parameters. Several techniques are employed to enhance the performance of the antenna after each design stage. A single patch antenna is initially designed to operate at 28 GHz while maintaining a wide bandwidth. An array technique is employed at the second stage (array-1) to enhance the bandwidth and gain of the preceding design. Minor improvements in the gain and bandwidth are achieved by increasing the number of identical array elements (array-2). The design is finalized (array with superstrate) by introducing a superstrate layer stacked above the patch array to enhance the overall gain of the antenna. The design for all proposed configurations is presented in Figure 1. Table 1 depicts the dimensions for the proposed geometries.

2.1. Single patch

A simple rectangular patch antenna is designed initially as shown in Figure 1a. In order to reduce antenna loss, it is implemented on low-loss Rogers RT/Duroid 5880 substrate with a thickness of 0.508 mm, dielectric

constant 2.2, and loss tangent 0.0009 [30, 31]. Copper is used as a metal on both sides of the substrate with a thickness of 0.035 mm and electrical conductivity 5.8e+007 S/m. The dimensions of the patch antenna can be calculated using the mathematical equations given in [8, 25].

The coaxial feed is used to excite the antenna that is positioned on the top right corner of the rectangular patch element to procure the good impedance matching, as illustrated in Figure 1a. The overall size for the single element patch antenna is 6 $\times$ 6 mm^2. The single element-based patch antenna achieves operational bandwidth of 4.36 GHz, ranging from 25.92 GHz to 30.28 GHz, and a peak gain of 8.25 dBi at 30.28 GHz. Further details and graphical analysis of the design are provided in Section 3.

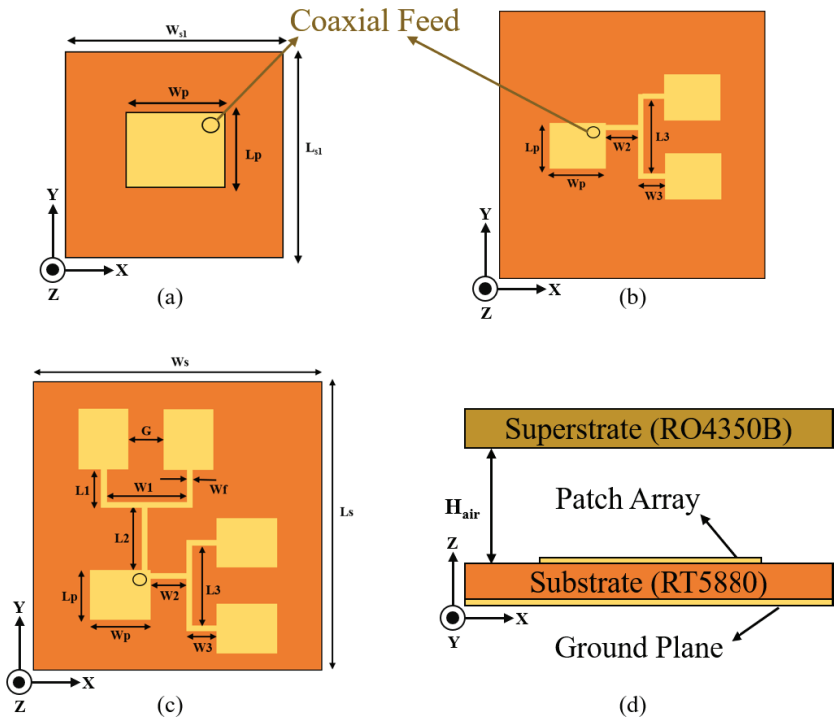

Figure 1. Proposed configurations of design: (a) single patch antenna, (b) array-1, (c) array-2, (d) array-2 with superstrate.

Table 1. Dimensions for all parameters (mm).

Parameters	Dimensions	Parameters	Dimensions
Ls=Ws	35	L2	9.35
Wp	4.2	L3	10.3
Lp	3.2	W1	10.3
Wf	0.7	W2	5.5
G	4.6	W3	6.2
L1	7.85	Ws1	6
H_{air}	5.4	Ls1	6

2.2. Array-1

An array technique is employed to enhance the peak gain and operational bandwidth as illustrated in Figure 1b. In addition to a single element, two elements are placed parallel to each other on the right side, resulting in a three-element array. For the excitation of additional array elements, a microstrip line of suitable dimensions is used. The array elements are added to enhance the resonant path, hence increasing the bandwidth [16]. An incremental bandwidth of 4.64 GHz is achieved with a peak gain of 9.94 dBi at 26.99 GHz.

2.3. Array-2

An array of five elements is proposed, as shown in Figure 1c, to get incremental peak gain and operational bandwidth. Two additional elements are placed on the upper side of array-1. A microstrip line is employed for the excitation of additional elements. An enhanced bandwidth of 4.78 GHz is achieved with a peak gain of 10.1 dBi at 26.99 GHz.

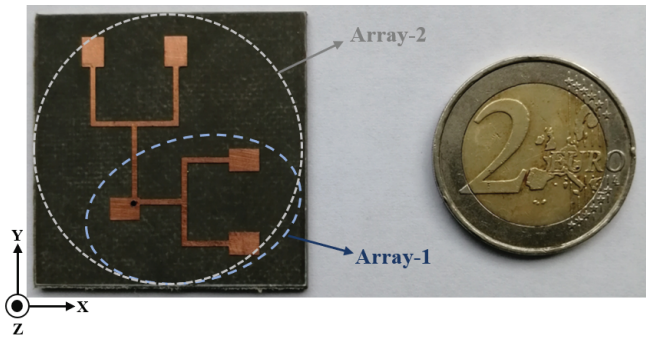

(a)

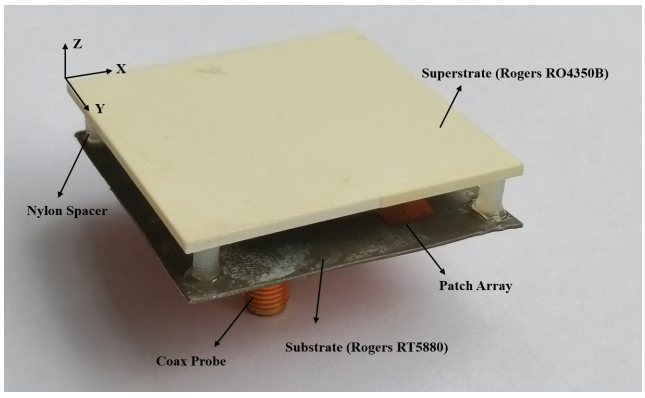

(b)

Figure 2. Fabricated prototype of the proposed array: (a) array-2 (front view without feed), (b) array-2 with superstrate (with coaxial feed).

2.4. Array-2 with superstrate

The superstrate layer is employed above the antenna array-2 to increase the antenna gain and efficiency as shown in Figure 1d. An inexpensive Rogers RO4350B material is used as a superstrate layer with a thickness of 1.524 mm, dielectric constant of 3.66, and loss tangent of 0.004 due to its property of low metallic losses at

the MMW band [32, 33]. The air gap between the superstrate layer and the antenna is usually taken to be about a half wavelength. Multiple reflections between the superstrate layer and the antenna lead to constructive interference that results in a high gain [19]. By adopting Rogers RO4350B as a superstrate, a peak gain of 13.4 dBi is achieved with a bandwidth of 5.4 GHz.

3. Results and discussion

This section presents the simulated results for all the proposed configurations and measured results for the fabricated prototype of array-2 with superstrate. The top view of the fabricated array-2 without the coaxial feed is depicted in Figure 2a. Nylon spacers are used to maintain the gap between the patch array layer and the superstrate (Rogers RO4350B), as illustrated in Figure 2b.

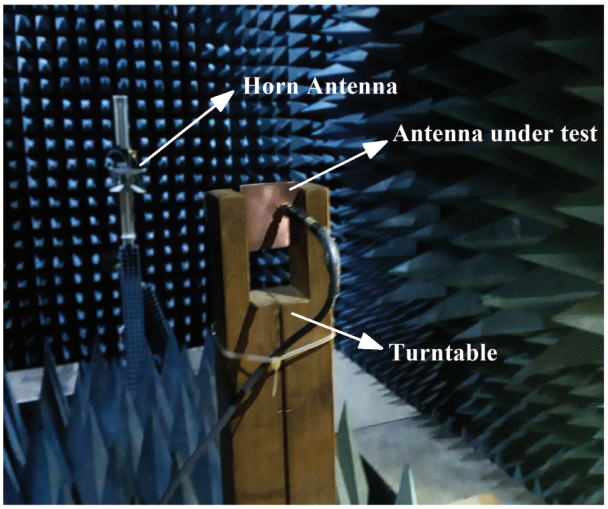

Figure 3. Antenna under test (AUT) in the far-field anechoic chamber.

The Rohde and Schwarz Vector Network Analyzer (VNA) ZNB40 and an anechoic environment are used to perform the measurements. The anechoic chamber provides a secure and controlled environment to test the antennas, as walls of the chamber are covered with pyramidal-shaped radiation absorbing material (RAM) that minimizes the reflected energy. Moreover, the anechoic chamber comprises a transmitting broadband horn antenna that directs the EM waves towards the antenna under test (AUT) that is mounted on a turntable in the far-field zone of a broadband horn antenna (probe), shown in Figure 3. The AUT is rotated in different orientations to obtain the radiation patterns in desired planes. Both simulated and measured results reveal excellent acquiescence regarding reflection coefficient, gain and radiation patterns. The simulated and measured results have minor discrepancies due to the fabrication tolerances and connector modeling [34].

3.1. Reflection coefficient

Figure 4a shows the reflection coefficient for all the proposed configurations of antenna design. A single patch antenna achieves a bandwidth of 4.36 GHz ranging from 25.92 to 30.28 GHz. For array-1, a bandwidth of 4.64 GHz ranging from 25.62 to 30.26 GHz is obtained. For array-2, a bandwidth of 4.78 GHz ranging from 25.38 to 30.16 GHz is realized. For array-2 with superstrate, a successful gain of 13.4 dBi is achieved with a wideband of 5.4 GHz ranging from 25.1 to 30.5 GHz, which is a good candidate for 5G.

3.2. Gain

Figure 4b shows simulated and measured results of gain for all the proposed configurations of the antenna. A single patch antenna, array-1, array-2, and array-2 with superstrate have achieved peak gain of 8.25 dBi, 9.94 dBi, 10.1 dBi, and 13.4 dBi at 30.28 GHz, 26.99 GHz, 26.99 GHz, and 27 GHz, respectively. A measured peak gain of 13.2 dBi is achieved.

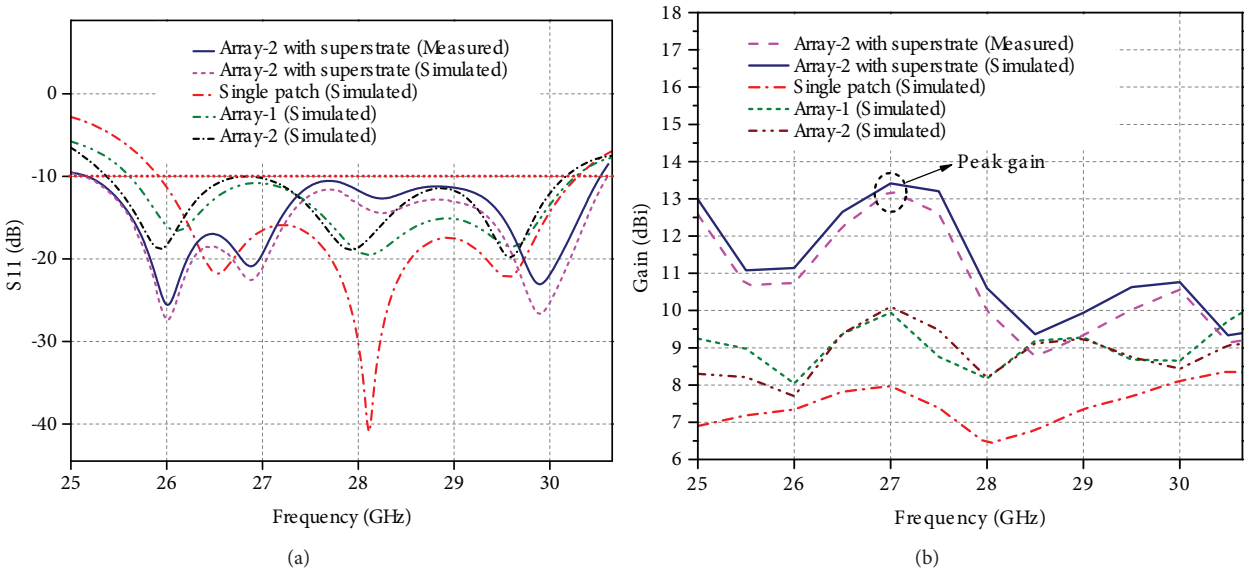

Figure 4. (a) Reflection coefficient (S11 parameter) for all the proposed configurations, (b) simulated and measured gain.

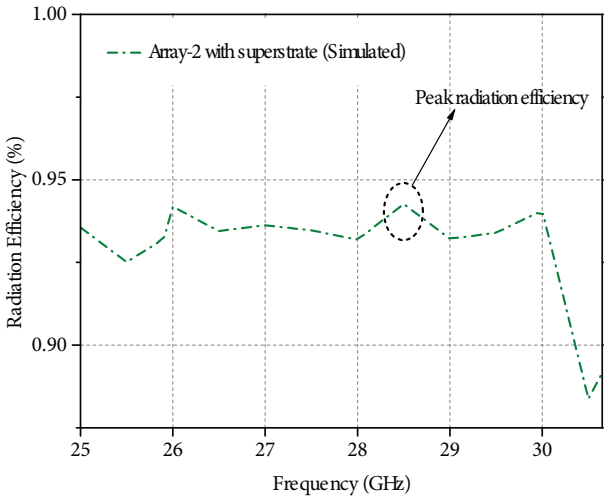

Figure 5. Simulated radiation efficiency.

3.3. Radiation efficiency

Figure 5 shows the simulated radiation efficiency. Array-2 with superstrate achieves simulated peak radiation efficiency of 94.2% at 28.5 GHz.

3.4. Radiation patterns

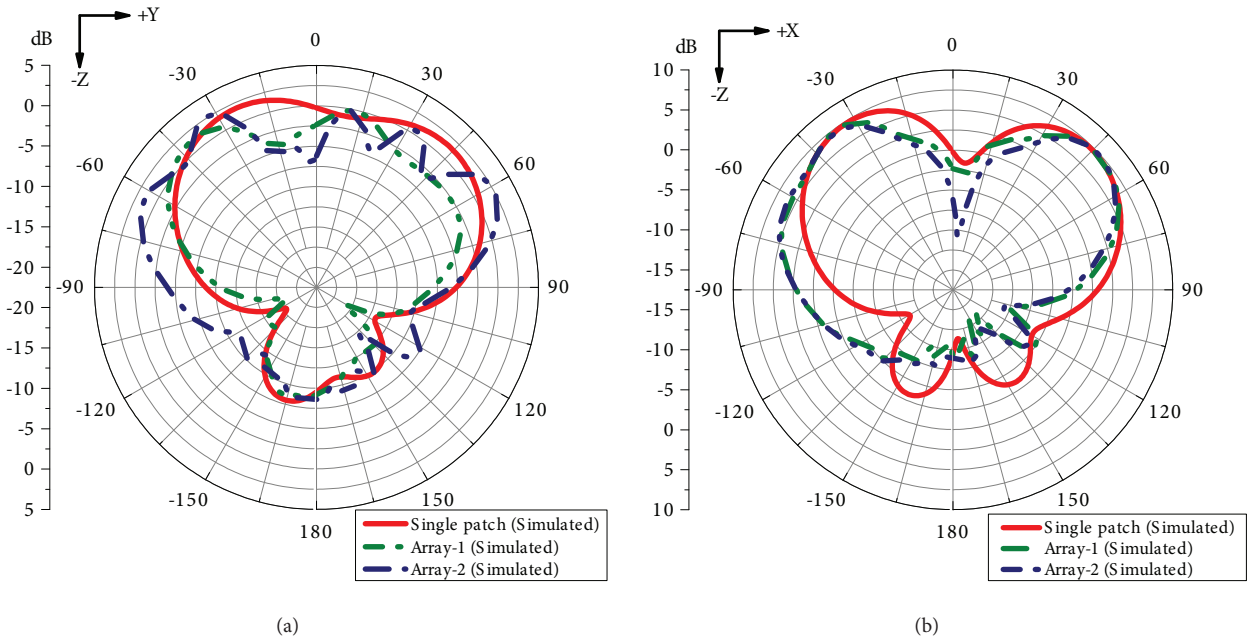

Figure 6. Radiation patterns at 25.9 GHz: (a) E-field, (b) H-field.

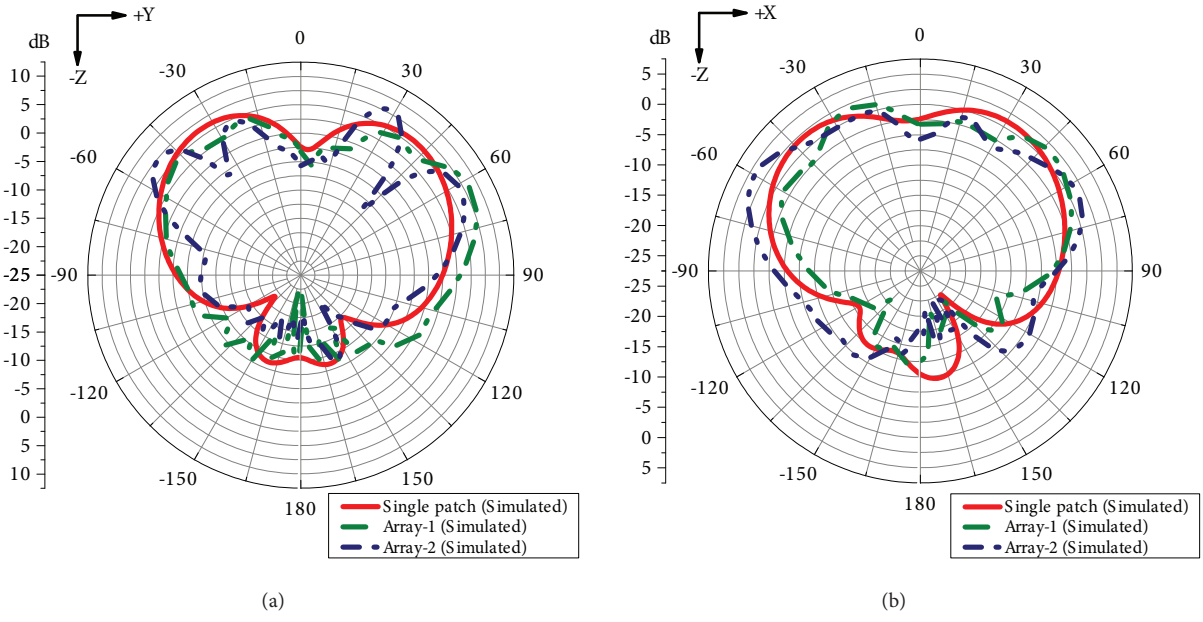

Figure 7. Radiation patterns at 29.5 GHz: (a) E-field, (b) H-field.

The simulated E-field radiation patterns (YZ plane; at ϕ=90°) for the initial three configurations of single patch antenna, array-1, and array-2 at 25.9 GHz are shown in Figure 6a. Moreover, the simulated H-field radiation patterns (XZ plane; at ϕ=0°) for the same configurations at 25.9 GHz are depicted in Figure 6b. Figures 7a and 7b depict the simulated E-field (YZ plane) and H-field (XZ plane) radiation patterns for the

first three configurations at 29.5 GHz. The simulated and measured E-field (YZ plane) and H-field (XZ plane) radiation patterns for array-2 with superstrate (fabricated prototype) at 27 GHz are shown in Figure 8a and Figure 8b, respectively.

From Figure 6 and Figure 7, it can be easily observed that the E-field radiation pattern of array-2 at 29.5 GHz is distorted as compared to the radiation pattern at 25.9 GHz. At 25.9 GHz H-field radiation patterns for the first three configurations are slightly split. Moreover, Figure 8a depicts that the E-field radiation pattern of array-2 with superstrate is unidirectional with reduced side lobe levels occurring at θ=34° and θ=-41°. Main lobe direction at θ=4° is obtained with a comparatively narrow beam that leads to high gain. Moreover, the H-field radiation pattern for array-2 with superstrate, shown in Figure 8b, is slightly distorted. The tested and simulated results show good agreement.

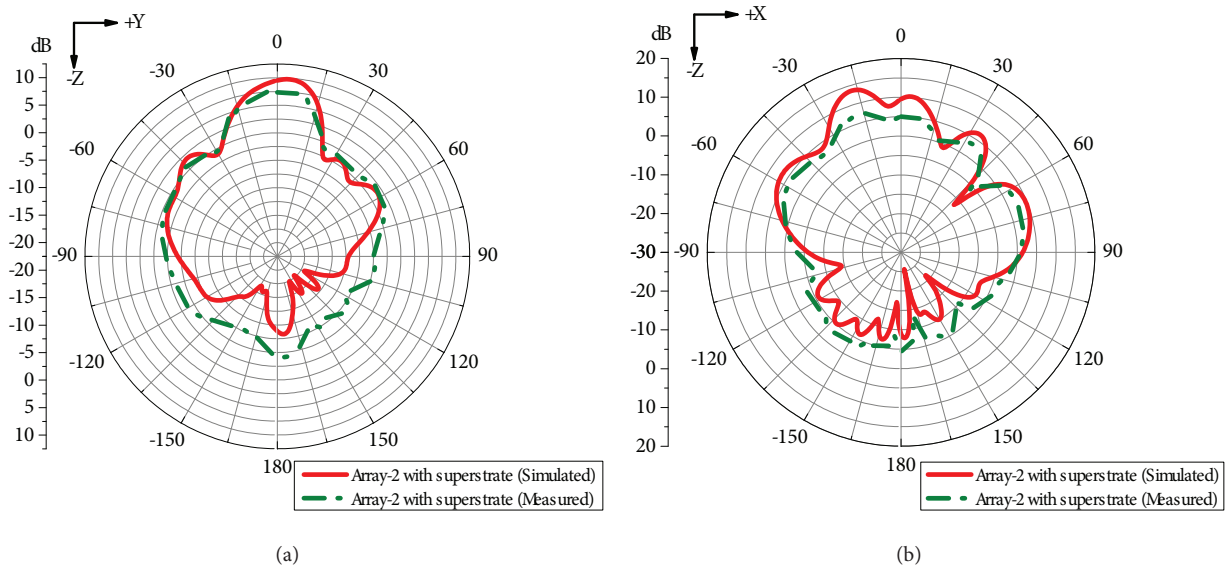

Figure 8. Radiation patterns at 27 GHz: (a) simulated and measured E-field, (b) simulated and measured H-field.

The 3-D gain pattern of the patch array antenna is provided in Figure 9. Gain peaks of up to 13.4 dBi are observed around the positive z axis, demonstrating good performance characteristics. Moreover, the antenna is designed to suppress the back lobes to efficiently radiate the electromagnetic waves towards the positive z axis.

The proposed design is compared with recently published works, as shown in Table 2. In [15], a wideband antenna is presented, which operates at low-frequency band (2.4 GHz) and high-frequency band (28 GHz) for LTE-A and 5G, respectively. The antenna occupies an area of 40 × 70 mm^2. A bandwidth of 2 GHz ranging from 27 to 29 GHz with gain of 9 dBi is achieved for the 5G band of 28 GHz at the expense of complicated structure and large size. In [20], an SIW-based array is presented. The overall size of the array is 72 × 27.4 × 0.508 mm^3 and it achieves a bandwidth of 4 GHz and a maximum gain of 12.1 dBi. In [21], another SIW-based antenna array is designed using three layers of substrate and a layer of copper. The fabricated antenna achieves a bandwidth of 2.3 GHz and a gain of 13.97 dBi. In [29], a broadband 2 × 2 dense dielectric patch antenna array is presented. The discussed design consists of two layers of substrates and a layer of the holey superstrate. The antenna array is excited through aperture coupling. A bandwidth of 4.3 GHz with a gain of 16 dBi is achieved to the detriment of complex structure. In [32], a multiband MIMO antenna is presented to cover the frequency bands for 4G and 5G. Two antennas that are connected in a linear manner are

Table 2. Comparison table (only for 5G antenna system).

References	Antenna substrate	Type	Feeding port(s)	Multilayer	Frequency band (GHz)	Bandwidth (GHz)	Gain (dBi)	Efficiency (%)	Size (mm^3)
[40]	RO3003	MIMO	2	✓	27.4–28.23	0.83	6.6	–	150 × 100 × 0.13
[22]	Nelco N9000	Three subarrays-based microstrip patch antenna	1	✗	21–22	1	13.5	–	55 × 110 × 4.5
[37]	RO3003	DRA MIMO	2	✓	30	1	8.6	80	48 × 21 × 4.13
[23]	–	Microstrip array	1	✓	26.83–28.56	1.73	21.4	–	74.5 × 89.55 × 1.07
[15]	RT Duroid 5880	SIW BM antenna with four chip antennas	8	✓	27–29	2	9	–	40 × 70 × 0.254
[26]	RT Duroid 5880	Patch array with shorting pins	1	✗	28.41–30.16	2.05	13	–	30.656 × 10 × 0.254
[5]	RT Duroid 5880	DRA array	1	✗	27–29.1	2.1	12.1	–	58 × 11 × 1.554
[21]	Rogers 4350B	Cavity backed aperture coupled array	1	✓	27.2–29.5	2.3	13.97	–	70 × 63.5 × 2.199
[35]	RO5880	Dipole array with via directors	1	✓	27–29.3	2.38	12.61	95.8	30 × 35.62 × 4.9
[36]	Taconic TLY-5	Patch array	1	✓	26.4–28.92	2.52	13.5	–	50.5 × 96.1 × 1.121
[38]	Rogers 5880	Vivaldi array	1	✗	24.55–28.5	3.95	11.32	–	60 × 28.823 × 0.787
[20]	Rogers Duroid 5880	Slot array	4	✗	28–32	4	12.1	–	72 × 27.4 × 0.508
[29]	Rogers Duroid 6002	Dielectic dense patch array	1	✓	26.5–30.8	4.3	16	92	22 × 24 × 7.056
[32]	RO4350B	MIMO	6	✗	25.7–30.5	4.8	9.9	–	115 × 65 × 0.76
[25]	RT Duroid 5880	Patch array	2	✗	24.4–29.3	4.9	10.29	71	110 × 75 × 0.508
[39]	Neltec	Dipole antennas with metamaterial	4	✗	26–31	5	10	–	31 × 48 × 0.254
This Work	RT Duroid 5880	Patch array	1	✓	25.1–30.5	5.4	13.4	94.2	35 × 35 × 7.43

responsible for attaining a 5G band. Moreover, four antenna elements are arranged in a MIMO configuration that is responsible for low-frequency bands. A peak gain of 9.9 dBi is achieved with a bandwidth of 4.8 GHz for 5G applications. In [35], an SIW-based 4 × 1 dipole antenna array with five layers of different thicknesses is proposed. The array achieves a bandwidth of 2.38 GHz with a gain of 12.61 dBi. In [36], a proximity coupled wideband antenna for 5G mobile communication achieves a bandwidth of 2.52 GHz at the cost of an enormous area (50.5 × 96.1 mm^2) and complex feeding mechanism. In [37], a two-linear-arrays-based MIMO antenna is proposed that attains a peak gain of 8.6 dBi with a bandwidth of 1 GHz at the cost of a large size. In [38], a eight-elements-based Vivaldi antenna is presented that achieves a bandwidth of 3.95 GHz with a maximum gain of 11.32 dBi. In [39], an array that is based on metamaterial unit cells is excited using two dipole antennas

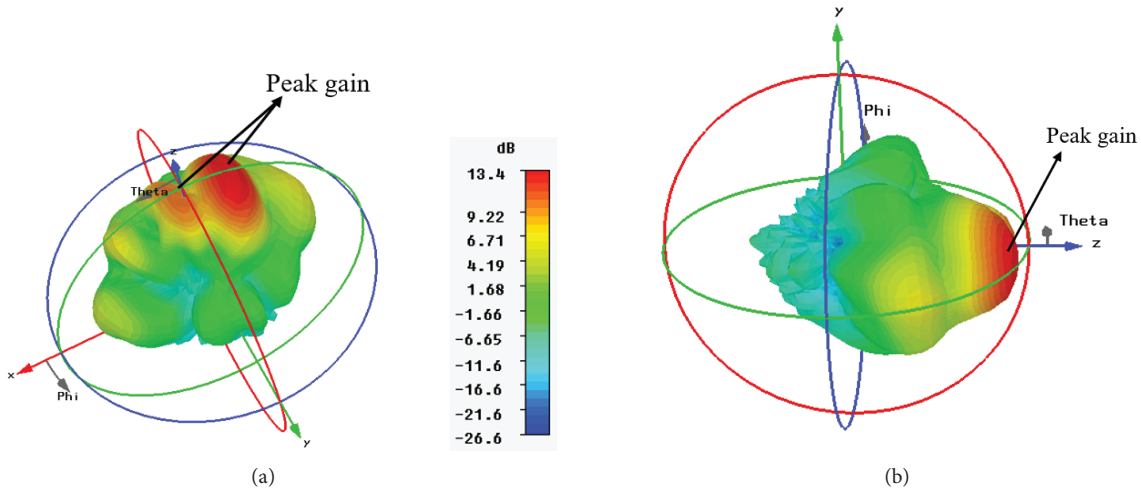

Figure 9. 3-D Gain pattern: (a) top view, (b) side view.

in a MIMO configuration. The presented antenna covers a wideband of 5 GHz ranging from 26 GHz to 31 GHz with peak gain of 10 dBi. In [40], the MIMO antenna based on two elements is designed for the 28 GHz band, and a peak gain of 6.6 dBi is achieved with a bandwidth of 0.83 GHz at the cost of enormous antenna size. In this work, a superstrate layer-based wideband antenna is proposed that covers the frequency band ranging from 25.1 to 30.5 GHz with a peak gain of 13.4 dBi.

4. Conclusions

In this work, a single rectangular patch antenna, two different configurations of patch arrays, and a finalized configuration of the patch array with superstrate are proposed, analyzed, and discussed. A single rectangular patch antenna is designed to achieve a bandwidth of 4.36 GHz with a peak gain of 8.25 dBi. An array configuration is employed to develop a five-element patch array structure resulting in a peak gain of 10.1 dBi with a bandwidth of 4.78 GHz. The superstrate layer is spaced above the antenna array to further enhance the gain. As a result, a peak gain of 13.4 dBi is achieved with a bandwidth of 5.4 GHz ranging from 25.1 GHz to 30.5 GHz for 5G applications. A simple coaxial feed is used for the excitation of the antenna. The proposed design holds potential for deployment in 5G applications owing to the offered advantages including wider bandwidth, high gain, lowered cost, and improved radiation efficiency while maintaining a compact physical footprint.

Authorship contributions

S.F. is responsible for the antenna design, fabrication, and manuscript preparation; F.A. is responsible for the antenna design and supervised the whole research; Y.A. is responsible for the antenna fabrication and measurements; J.L. analyzed the acquired data and the results, revised the manuscript, and provided intellectual suggestions.

References

[1] Agiwal M, Roy A, Saxena N. Next generation 5G wireless networks: a comprehensive survey. IEEE Communications Surveys & Tutorials 2016; 18: 1617-1655.

[2] Garcia-Marin E, Masa-Campos JL, Sanchez-Olivares P. Diffusion bonding manufacturing of high gain W-band antennas for 5G applications. IEEE Communications Magazine 2018; 56: 21-27.

[3] Mahmoud KR, Montaser AM. Optimised 4 × 4 millimetre wave antenna array with DGS using hybrid ECFO-NM algorithm for 5G mobile networks. IET Microwaves, Antennas & Propagation 2017; 11: 1516-1523.

[4] Jilani SF, Alomainy A. A multiband millimeter-wave 2-D array based on enhanced franklin antenna for 5G wireless systems. IEEE Antennas and Wireless Propagation Letters 2017; 16: 2983-2986.

[5] Nor NM, Jamaluddin MH, Kamarudin MR, Khalily M. Rectangular dielectric resonator antenna array for 28 GHz applications. Progress In Electromagnetics Research C 2016; 63: 53-61.

[6] Bai X, Qu S, Ng KB, Chan CH. Center-fed patch antenna array excited by an inset dielectric waveguide for 60-GHz applications. IEEE Transactions on Antennas and Propagation 2016; 64: 1733-1739.

[7] Yang X, Ge L, Wang J, Sim C. A differentially driven dual-polarized high-gain stacked patch antenna. IEEE Antennas and Wireless Propagation Letters 2018; 17: 1181-1185.

[8] Balanis CA. Antenna Theory: Analysis and Design. 2nd Ed. Hoboken, NJ, USA; Wiley-Interscience, 1997.

[9] Elmezughi AS, Rowe WST, Waterhouse RB. Edge-fed cavity backed patch antennas and arrays. IET Microwaves, Antennas & Propagation 2009; 3: 614-620.

[10] Yang W, Wang H, Che W, Wang J. A wideband and high-gain edge-fed patch antenna and array using artificial magnetic conductor structures. IEEE Antennas and Wireless Propagation Letters 2013; 12: 769-772.

[11] Jilani SF, Alomainy A. Millimetre-wave T-shaped MIMO antenna with defected ground structures for 5G cellular networks. IET Microwaves, Antennas & Propagation 2018; 12: 672-677.

[12] Wei K, Li J, Wang L, Xu R. Microstrip antenna array mutual coupling suppression using coupled polarisation transformer. IET Microwaves, Antennas & Propagation 2017; 11: 1836-1840.

[13] Umar Khan Q, Bin Ihsan M, Fazal D, Mumtaz Malik F, Amin Sheikh S et al. Higher order modes: a solution for high gain, wide-band patch antennas for different vehicular applications. IEEE Transactions on Vehicular Technology 2017; 66: 3548-3554.

[14] Han W, Yang F, Ouyang J, Yang P. Low-cost wideband and high-gain slotted cavity antenna using high-order modes for millimeter-wave application. IEEE Transactions on Antennas and Propagation 2015; 63: 4624-4631.

[15] Lee C, Khattak MK, Kahng S. Wideband 5G beamforming printed array clutched by LTE-A 4 × 4-multiple-input multiple-output antennas with high isolation. IET Microwaves, Antennas & Propagation 2018; 12: 1407-1413.

[16] Cheng C, Chen J, Su H, Lin K. A wideband square-slot antenna array with superstrate and electromagnetic bandgap reflector for 60-GHz applications. IEEE Transactions on Antennas and Propagation 2017; 65: 4618-4625.

[17] Dadgarpour A, Sharifi SM, Kishk AA. Wideband low-loss magnetoelectric dipole antenna for 5G wireless network with gain enhancement using meta lens and gap waveguide technology feeding. IEEE Transactions on Antennas and Propagation 2016; 64: 5094-5101.

[18] Vosoogh A, Kildal P, Vassilev V. Wideband and high-gain corporate-fed gap waveguide slot array antenna with ETSI Class II radiation pattern in V-band. IEEE Transactions on Antennas and Propagation 2017; 65: 1823-1831.

[19] Asaadi M, Afifi I, Sebak A. High gain and wideband high dense dielectric patch antenna using FSS superstrate for millimeter-wave applications. IEEE Access 2018; 6: 38243-38250.

[20] Yang Q, Ban Y, Kang K, Sim C, Wu G. SIW multibeam array for 5G mobile devices. IEEE Access 2016; 4: 2788-2796.

[21] Park S, Shin D, Park S. Low side-lobe substrate-integrated-waveguide antenna array using broadband unequal feeding network for millimeter-wave handset device. IEEE Transactions on Antennas and Propagation 2016; 64: 923-932.

[22] Ojaroudiparchin N, Shen M, Zhang S, Pedersen GF. A switchable 3-D-coverage-phased array antenna package for 5G mobile terminals. IEEE Antennas and Wireless Propagation Letters 2016; 15: 1747-1750.

[23] Dzagbletey PA, Jung Y. Stacked microstrip linear array for millimeter-wave 5G baseband communication. IEEE Antennas and Wireless Propagation Letters 2018; 17: 780-783.

[24] Haraz OM, Elboushi A, Alshebeili SA, Sebak A. Dense dielectric patch array antenna with improved radiation characteristics using EBG ground structure and dielectric superstrate for future 5G cellular networks. IEEE Access 2014; 2: 909-913.

[25] Naqvi SI, Naqvi AH, Arshad F, Riaz MA, Azam MA et al. An integrated antenna system for 4G and millimeter-wave 5G future handheld devices. IEEE Access 2019; 7: 116555-116566.

[26] Jian R, Chen Y, Chen T, Li Z. Efficient design of compact millimeter wave microstrip linear array with bandwidth enhancement and sidelobe reduction. International Journal of RF and Microwave Computer-Aided Engineering 2019; 21881: 1-20.

[27] Joshi K, Saraswat S, Gulati G, Tiwari V. Superstrate layer in patch antenna - a review. International Journal of Latest Trends in Engineering Technology 2015; 6: 1-15.

[28] Zeb BA, Hashmi RM, Esselle KP. Wideband gain enhancement of slot antenna using one unprinted dielectric superstrate. Electronics Letters 2015; 51: 1146-1148.

[29] Asaadi M, Sebak A. Gain and bandwidth enhancement of 2 $\times$ 2 square dense dielectric patch antenna array using a holey superstrate. IEEE Antennas and Wireless Propagation Letters 2017; 16: 1808-1811.

[30] Mao C, Gao S, Wang Y. Broadband high-gain beam-scanning antenna array for millimeter-wave applications. IEEE Transactions on Antennas and Propagation 2017; 65: 4864-4868.

[31] Mahmoud KR, Montaser AM. Performance of tri-band multi-polarized array antenna for 5G mobile base station adopting polarization and directivity control. IEEE Access 2018; 6: 8682-8694.

[32] Ikram M, Sharawi MS, Shamim A, Sebak A. A multiband dual standard MIMO antenna system based on monopoles (4G) and connected slots (5G) for future smart phones. Microwave and Optical Technology Letters 2018; 60: 1468-1476.

[33] Zhai W, Miraftab V, Repeta M. Broadband antenna array with low cost PCB substrate for 5G millimeter wave applications. In: IEEE Global Symposium on Millimeter-Waves; Montreal, Canada; 2015. pp. 1-3.

[34] Gupta S, Briqech Z, Sebak A, Ahmed Denidni T. Mutual-coupling reduction using metasurface corrugations for 28 GHz MIMO applications. IEEE Antennas and Wireless Propagation Letters. 2017; 16: 2763-2766.

[35] El-Halwagy W, Mirzavand R, Melzer J, Hossain M, Mousavi P. Investigation of wideband substrate-integrated vertically-polarized electric dipole antenna and arrays for mm-Wave 5G mobile devices. IEEE Access 2018; 6: 2145-2157.

[36] Diawuo HA, Jung YB. Wideband proximity coupled microstrip linear array design for 5G mobile communication. Microwave and Optical Technology Letters 2017; 59: 2996-3002.

[37] Sharawi MS, Podilchak SK, Hussain MT, Antar YMM. Dielectric resonator based MIMO antenna system enabling millimetre-wave mobile devices. IET Microwaves, Antennas & Propagation 2017; 11: 287-293.

[38] Zhu S, Liu H, Chen Z, Wen P. A compact gain-enhanced Vivaldi antenna array with suppressed mutual coupling for 5G mmWave application. IEEE Antennas and Wireless Propagation Letters 2018; 17: 776-779.

[39] Wani Z, Abegaonkar MP, Koul SK. A 28-GHz antenna for 5G MIMO applications. Progress In Electromagnetics Research Letters 2018; 78: 73-79.

[40] Ikram M, Sharawi MS, Klionovski K, Shamim A. A switched beam millimeter wave array with MIMO configuration for 5G applications. Microwave and Optical Technology Letters 2018; 60: 915-920.